

Zone-edge phonons in mixed zinc-sulfide-zinc-selenide crystals

D. Schmeltzer, R. Beserman, and D. Slamovits

Solid State Institute, Technion-Israel Institute of Technology, Haifa, Israel
and Department of Physics, Technion-Israel Institute of Technology, Haifa, Israel

(Received 27 August 1979)

The vibrational properties of zinc-sulfide-zinc-selenide zone-edge phonons (ZEP) have been studied using infrared absorption and Raman scattering. The ZEP behavior cannot be described in the usual one-two modes framework; it has been observed that, when the S content decreases the ZnS ZEP tend towards the S-localized mode in ZnSe; when Se content decreases, the LO (ZnSe) phonons at the X point of the Brillouin zone tend towards the LA (ZnS) frequencies at the same points and no mixing between ZnS and ZnSe phonons is seen. In the range of acoustic frequencies, the ZnS disorder-induced TA mode is Raman active, as are the 2TA (ZnS) and 2TA (ZnSe) frequencies without crossed mixing. Two types of vibrations are observed: a localized one and a propagating one whose frequency is close to that of the virtual-lattice phonon.

INTRODUCTION

Until now most of the experimental and theoretical work on mixed crystals has been devoted to the study of the vibrational properties of phonons in the center of the Brillouin zone (BZ).¹ It has been found that two major classes of behavior can be observed: *one-mode* behavior for which the zone-center-phonon (ZCP) frequencies vary continuously with the impurity concentration and *two-mode* behavior for which two oscillators corresponding to the two constituents exist for all concentrations.

In order to understand to what extent the phonon eigenstates can be described by plane waves, and how this concept can be projected into the BZ, it is necessary to learn not only what happens in the center of the BZ but in all directions and for all the values of the BZ. *A priori*, the experimental technique which best fits this goal is neutron diffraction.

Few experiments have been performed using this technique. Diffraction by $\text{NHCl}_{1-x}\text{Br}_x$ (Ref. 2) showed a mixing of different optical and acoustical branches leading to broad incoherent bands related to the phonon density of states. These bands could not be followed throughout the entire composition range of the mixture; the onset of disorder due to the mixing caused a considerable broadening in the region where there should be a lifting of the degeneracy at the band-mode crossing with the TA and LA branches. It has been shown that the presence of a gap impurity mode in the two-mode-type crystal $\text{ZnS}_x\text{Se}_{1-x}$ with x or $1-x=0.25$, does not appreciably affect the host-lattice density of states. On the other hand, in the one-mode-type crystal $\text{ZnSe}_x\text{Te}_{1-x}$ with $1-x=0.25$, the phonon density of states is that of a virtual crystal, the average of the two components.³ Unfortunately

these experiments have not been performed in mixed crystals with higher-impurity concentration and no generalization can be proposed unambiguously.

Phonons with opposite momenta can be coupled together to give zero momentum. The standing wave can absorb or reflect the infrared light (ir) or can Raman scatter (RS) the incoming laser light.^{4,5} The momentum region which will be "seen" by these techniques will mainly be the zone-edge region where the phonon density of states is high.

Zinc-sulfide-zinc-selenide mixed crystals are ideal materials for this study. They are transparent to the 6471-Å krypton laser light which excludes resonant effects and they do not contain free carriers which permit observation of the ir-absorption processes by coupled phonons.

In addition, some experimental information is already available on ZnS, ZnSe, and their mixture. The zone-edge phonons of the pure components have been studied⁶⁻⁸ using ir absorption. More recently, second-order Raman-scattering experiments were performed on ZnS (Ref. 9) and ZnSe (Ref. 10). Neutron-diffraction data of great accuracy for ZnS (Ref. 11) and of less accuracy for ZnSe (Ref. 12) are available now and will be used to fit our experimental data.

The optical properties of mixed zinc sulfide-zinc selenide have been studied in the center of BZ.¹³ Because S in ZnSe and Se in ZnS generate nonpropagating impurity modes, $\text{ZnS}_{1-x}\text{Se}_x$ crystals have a typical two-mode behavior with two TO_Γ and LO_Γ modes for all impurity concentrations.

The first theoretical attempt to understand zone-edge phonons (ZEP) in this type of crystal was based on an extension of a simple random-element isodisplacement model.¹⁴ According to this theory $\text{ZnS}_{1-x}\text{Se}_x$ should exhibit a mixture of one- and

two-mode behavior for optical and acoustical ZEP.

In the next section we analyze the double-phonon processes of pure ZnS and ZnSe taking into account the neutron scattering data. The third section will be devoted to the ir and Raman study of mixed $\text{ZnS}_{1-x}\text{Se}_x$. The experimental results will be discussed in the last section.

EXPERIMENTAL RESULTS

A. Identification of the ZnS and ZnSe double phonon

Infrared-absorption measurements on polycrystalline material were performed at room temperature using a Beckman double spectrometer. The selection rules which govern the combination of ZEP in crystals with zinc-blende structure have been established for different directions and for some specific points of the BZ.⁹ They are based on Birman's calculation.^{15,16}

Figure 1 shows the ir-absorption coefficient of ZnS and ZnSe. The double-phonon absorption spectra extend from the reststrahlen LO frequency to two times the highest frequency of the optical phonons.

The absorption peaks of pure ZnS and ZnSe have been assigned to the combinations of optical and acoustical phonons with opposite momenta as presented in Table I. This assignment is based on the frequencies deduced from neutron scattering experiments.^{11,12} In pure ZnS the high-frequency-absorption peaks are generated only by the addition of two optical phonons, 2LO_L , 2TO_X , and 2TO_E ; the other peaks are due to the addition of optical and acoustical phonons. In the Σ direction, the splitting between the TO branches generates

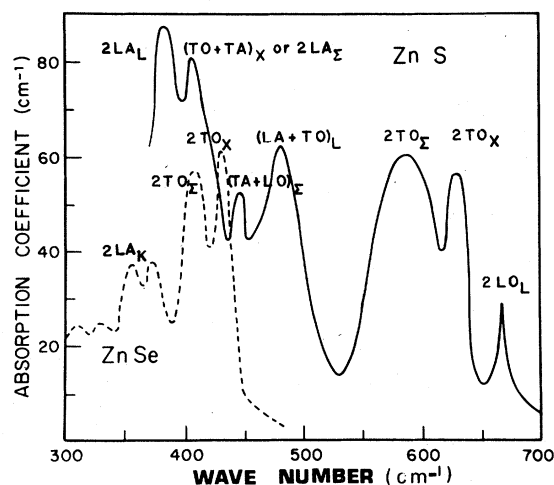


FIG. 1. Infrared-absorption coefficient of pure ZnS and ZnSe.

TABLE I. Double-phonon assignments.

Frequencies (cm^{-1})	Assignments
(a) ZnS 667	2LO_L
630	2TO_X
585	2TO_E
480	$\text{LA}_L + \text{TO}_L$
440	$\text{TA}_E + \text{TO}_E$
404	$\text{TO}_X + \text{TA}_X$ or 2LA_E
386	2LA_L
(b) ZnSe 430	2TO_X or $(\text{LO}_X + \text{TO}_X)$
410	2TO_E
370	$\text{LA}_L + \text{LO}_L$
354	2LA_K
330	2LA_L

a broad band whose maximum is 585 cm^{-1} .

Our experimental results on ZnS are in agreement with Deutsch's¹⁶ findings with the exception of the higher-order combination processes which have not been seen in the present work. Our assignments differ because at the time when Deutsch's experiment was performed neither the neutron data nor the selection rules were published.

Because of the small difference in mass between zinc and selenium, the frequency difference between the LO and the LA branches is small at the edges of ZnSe BZ. Consequently, there are not regions of the ir spectrum which can be attributed to combinations of optical phonons only. For each ir-absorption peak there will be more than one possible combination process. In addition, there are fewer neutron data for ZnSe than for ZnS. The assignment proposed in Table I can nevertheless be made, giving the best fit with the known neutron results. This attribution differs from that previously published but our interpretation takes into account the fact that a crossing between TO and LO branches takes place in the X and L points of the BZ.^{12,17}

Our RS results on ZnS and ZnSe are in good agreement with previously published results. As compared to ir, the RS experiment does not give any additional information on the optical branches, but it is more sensitive and accurate in the acoustical energy range. Therefore, we shall make use preferentially of the ir data for the optical branches and of RS for the acoustical branches.

B. Infrared absorption by $\text{ZnSe}_{1-x}\text{S}_x$

ir measurements were performed on polycrystalline $\text{ZnSe}_{1-x}\text{S}_x$ samples about 0.5 mm thick. The frequency dependence of the ZEP in the range of two times the ZnS optical phonon has been followed

as a function of x . In this frequency range the ir-absorption peaks are only generated by the ZnS-like combinations of phonons. The ZnSe range coincides with the tail of the ZnS reststrahlen, the absorption coefficient of which is much higher than the two-phonon absorption processes and partially masks them.

Figure 2 shows the absorption coefficient of some mixed crystals: $\text{ZnS}_{0.95}\text{Se}_{0.05}$, $\text{ZnS}_{0.75}\text{Se}_{0.25}$, $\text{ZnS}_{0.50}\text{Se}_{0.50}$, and $\text{ZnS}_{0.25}\text{Se}_{0.75}$. The highest frequency peak of ZnS is the 2LO_L overtone; its intensity decreases very rapidly with decreasing $1-x$ and is not seen when $1-x \leq 0.75$. In ZnS, where the mass ratio between Zn and S is 2, the longitudinal-optical branches are generated mainly by the displacement of the light sulfur atoms. The phonon density of states at the point L is expected to decrease roughly as the S concentration at least for small $(1-x)$ values. When Se is introduced, the light ion which was S in ZnS becomes Zn in ZnSe. The disorder which is created is not only proportional to the decrease of the number of S ions, but also to the fact that Zn is partially the light component in $\text{ZnS}_{1-x}\text{Se}_x$. This disorder, which results in an ill-defined LO_L phonon, does not strongly affect the TO branches, the eigenvectors of which are combinations of the S and Zn eigenvectors. With increasing Se content the TO and LO branches of ZnS merge into a single nondispersive branch at 295 cm^{-1} , which corresponds to the localized vibration of S in ZnSe. With increasing Se content, the double-optical-phonon

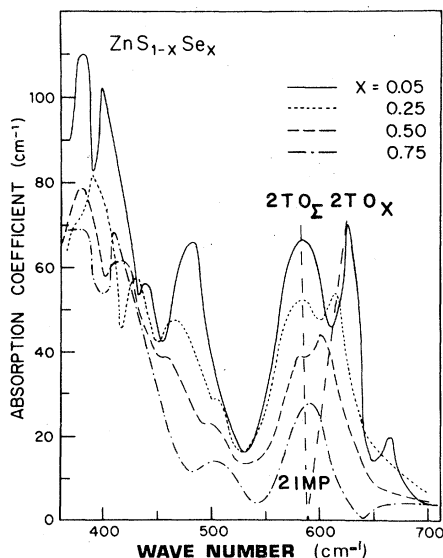


FIG. 2. Infrared-absorption coefficient of mixed $\text{ZnS}_{1-x}\text{Se}_x$, $x=0.05, 0.25, 0.5, \text{ and } 0.75$; the dotted line represents the frequency shift of the ZnS double-phonon peaks as a function of concentration.

bandwidth decreases because the frequency difference between the optical branches decreases, and its intensity decreases with the ZnS density of state. The absorption peaks in the frequency range 450 cm^{-1} – 500 cm^{-1} cannot be attributed to combinations of ZnS and ZnSe optical phonons, since this would result in an increase of the absorption coefficient with S(Se) content up to a maximum value for $\text{ZnS}_{0.5}\text{Se}_{0.5}$, which is not the case. We attribute the peak in the vicinity of 500 cm^{-1} to the $(\text{TO}_L + \text{LA}_L)(\text{ZnS})$. This peak has a frequency which shifts toward higher values as S content decreases because: (a) The $\text{LA}_L(\text{ZnS})$ (192 cm^{-1}) is transformed into the $\text{LO}_L(\text{ZnSe})$ (222 cm^{-1}) which results in a slight shift towards higher frequencies; (b) the $\text{TO}_L(\text{ZnS})$ (286 cm^{-1}) shifts towards the S-localized mode in ZnSe (295 cm^{-1}). In the frequency range smaller than 440 cm^{-1} contributions from both ZnS and ZnSe are ir active, which make the identification difficult. Nevertheless, for small enough concentrations of S in ZnSe, the absorption spectrum is mainly composed of ZnSe-phonon combinations, and a broadening of 2TO and 2LA branches of ZnSe takes place. When S is the major component in the mixture, the double-phonon absorption spectrum is washed out by the ZnS-reststrahlen absorption band.

C. Raman scattering of $\text{ZnS}_{1-x}\text{Se}_x$

RS spectra of mixed polycrystalline samples were obtained with a Spex triple monochromator; the excitation source was the 6471-\AA line of a krypton laser.

In Fig. 3 the room-temperature spectra of ZnS, $\text{ZnS}_{0.5}\text{Se}_{0.5}$, and ZnSe are shown. The ZnS and ZnSe are identical to those previously published. When ZnS and ZnSe are mixed, we observe a two-mode behavior for the optical branches and no combinations between zone-edge ZnS optical phonons, which is consistent with the ir results. A two-mode behavior of the acoustical branches is observed which will be examined in more detail. Crossed combinations between zone-center phonons can only be seen under resonant RS conditions.¹⁸

Figure 4 shows the low-frequency RS spectra of ZnS, $\text{ZnS}_{0.75}\text{Se}_{0.25}$, $\text{ZnS}_{0.50}\text{Se}_{0.50}$, $\text{ZnS}_{0.25}\text{Se}_{0.75}$, and ZnSe. The RS of pure ZnS and ZnSe has already been studied in detail, both as a function of the polarization conditions^{9,10} and as a function of hydrostatic pressure.¹⁹ The low-frequency part of the ZnS spectra is composed mainly of two peaks at 182 and 218 cm^{-1} ; the first one has been attributed to 2TA_x and the second one to $\text{TO}_L - \text{TA}_L$. The spectrum of ZnSe is composed of the zone-center phonons TO_T and LO_T at 205 and

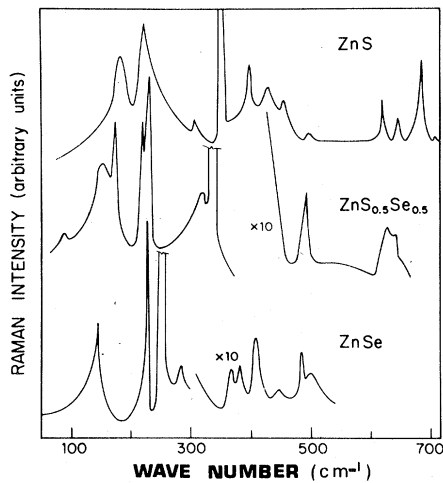


FIG. 3. Raman spectra of ZnS, $\text{ZnS}_{0.5}\text{Se}_{0.5}$; the laser excitation is the 6471-Å line.

250 cm^{-1} , respectively. The intense band at 142 cm^{-1} contains two coupled modes: 2TA_x and $\text{TO}_L - \text{TA}_L$ which split apart when hydrostatic pressure is applied; the 2TA_x peak is more intense than that of the $\text{TO}_L - \text{TA}_L$.

When 25% of ZnSe is introduced into ZnS, the shape of the double-phonon spectrum is strongly modified. The impurity mode of ZnSe is in the frequency range of $(\text{TO}_L - \text{TA}_L)(\text{ZnS})$ and results in the disappearance of this double-phonon frequency and in an increased intensity of the $2\text{TA}_x(\text{ZnS})$ peak. These effects could be the result of an interference between the continuum of double phonons and the localized impurity gap mode.²⁰

The $\text{ZnS}_{0.5}\text{Se}_{0.5}$ mixed-crystal low-frequency spectrum is composed of the ZnSe-like zone-center phonons, which split apart from the Se-gap mode and of the shifted $2\text{TA}_x(\text{ZnS})$ and $2\text{TA}_L(\text{ZnSe})$ peaks. An additional peak at 83 cm^{-1} appears which has been attributed to the disorder-induced one-phonon density of state, and fits well the TA (ZnS) frequency.²¹ The acoustical peaks do not shift appreciably with impurity concentration. No ZnSe-disorder-induced mode has been seen; this will be discussed later together with the fact that the ZnS-disorder-induced peaks appear for $1 - x \leq 0.5$.

The RS spectrum of $\text{ZnS}_{0.25}\text{Se}_{0.75}$ shows a decrease of the zone-center ZnSe-like phonon intensities with respect to the double-phonon band which is split into two main peaks at 150 and 172 cm^{-1} . The former, which is more intense, is related to ZnSe, and the latter to ZnS.

DISCUSSION

The absence of cross coupling between ZnS and ZnSe ZEP, the appearance of a ZnS-induced TA

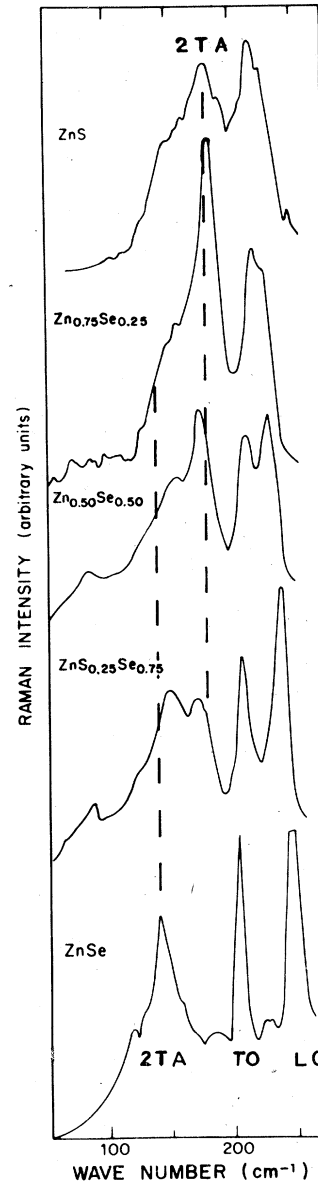


FIG. 4. $\text{ZnS}_{1-x}\text{Se}_x$ low-frequency Raman spectra: $x=0$, 0.25, 0.5, 0.75, and 1.

peak in a crystal where ZnS concentration is smaller than 50%, as well as the existence of two TA branches, can be understood in the following framework.

The virtual-crystal model can be applied to the TA branches; it predicts normal modes of vibration, the frequencies of which are the average of the ZnSe and ZnS branches. In addition, for low enough concentrations of ZnS, a TA mode corresponding to the vibration of the Zn generates a localized vibration which is momentum independent. For the propagating phonon, spatial coherence be-

tween vibrations exists, which allows combinations of phonons with opposite momenta. As for the localized mode, no selection rules hold and second-order RS is possible. These two types of phonons are not of the same nature and therefore cannot be cross coupled. The localized mode with its momentum-independent frequency can interact with light.

In this model the characteristic equation is written²²

$$\omega^2 u_{\alpha,l} - \sum_{\alpha',l'} \langle D_{\alpha,l,\alpha',l'} \rangle u_{\alpha',l'} = \frac{\partial}{\partial u_{\alpha,l}} F(V - \langle V \rangle), \quad (1)$$

where V is the usual potential:

$$\langle V \rangle = \frac{1}{2} \sum_{\alpha,l,\alpha',l'} \langle D_{\alpha,l,\alpha',l'} \rangle u_{\alpha,l} u_{\alpha',l'}. \quad (2)$$

In a crystal which does not contain disorder, D is the usual dynamical matrix, the nonlinear function does not act on the first term of the characteristic equation, and the solutions are those of a virtual crystal.

When the disorder is introduced, Eq. (1) has two sets of eigenfrequencies. The first occurs when the frequency ω has a value within the range of the virtual-lattice frequencies; the nonlinear part of the characteristic equation does not modify the nature of the propagating mode. The second occurs when ω has a value which is above the maximum value of the virtual crystal and new solutions are found corresponding to nonpropagating phonons. The departure from the virtual crystal can be written in the case of $\text{ZnS}_{0.50}\text{Se}_{0.50}$ as follows:

$$V - \langle V \rangle = \frac{1}{2} \sum K \Delta_1 u_{2,l}^2 - 2G \Delta_2 u_{2,l} (u_{1,l} + u_{1,l+1}) - (K - G) u_{2,l} u_{1,l}. \quad (3)$$

In the unit l the Zn atoms occupy the site 1 and the S(Se) occupy the site 2:

$$\Delta_1 = \frac{1}{2} \left(\frac{1}{m_s} - \frac{1}{m_{se}} \right),$$

$$\Delta_2 = \frac{1}{2} \left(\frac{1}{\sqrt{m_s}} - \frac{1}{\sqrt{m_{se}}} \right) \frac{1}{\sqrt{m_{zn}}}, \quad (4)$$

where K and G are, respectively, the coupling constants within the l cell and from the l to $(l+1)$ cell.

We want to evaluate $V - \langle V \rangle$ in $\text{ZnS}_{1-x}\text{Se}_x$. K and G will be expressed, respectively, as the sum of and the difference between two force constants A and B , which will be deduced from the experimental frequencies of ZnS and ZnSe at the X point; A and B are concentration independent. At the

edge of the BZ the frequencies and the displacement vectors are given by the solution to

$$\begin{pmatrix} \omega^2 - \frac{4A}{M_1} & \frac{4B}{M_2} \\ \frac{4B}{M_1} & \omega^2 - \frac{4A}{M_2} \end{pmatrix} \begin{pmatrix} \bar{l}_1 \\ \bar{l}_2 \end{pmatrix} = 0. \quad (5)$$

The transverse frequencies are

$$\omega_{\text{TO,TA}}^2 = 2A \left(\frac{1}{M_1} + \frac{1}{M_2} \right) \pm [4A^2(M_1^{-1} - M_2^{-1})^2 + 16B^2 M_1^{-1} M_2^{-1}]^{1/2}. \quad (6)$$

The displacements are

$$\Psi_{\text{TO}} = \frac{1}{2} (\bar{l}_1 - \bar{l}_2), \quad (7)$$

$$\Psi_{\text{TA}} = \frac{1}{2} (\bar{l}_1 + \bar{l}_2).$$

At the X point the longitudinal frequencies correspond to the linear chain with only the force constant $A \neq 0$, and $B = 0$.

From the $\text{TO}_X(\text{ZnSe}) = 215 \text{ cm}^{-1}$ and $\text{TA}_X(\text{ZnSe}) = 70 \text{ cm}^{-1}$ we can deduce A and B (in a.u.)

$$A = 4.6 \times 10^5 \text{ sec}^{-2},$$

$$B = 3.7 \times 10^5 \text{ sec}^{-2}$$

for a mixed crystal $\text{ZnS}_{0.5}\text{Se}_{0.5}$. The virtual-crystal frequency is given by Eq. (6) with

$$\frac{1}{m_2} = \frac{1}{2} \left(\frac{1}{m_s} + \frac{1}{m_{se}} \right).$$

The calculated frequency $\omega_{\text{TA}} = 72 \text{ cm}^{-1}$ is in good agreement with our experimental value $\text{TA}_X = 78 \text{ cm}^{-1}$.

The localized frequency is deduced from Eq. (3) which is more conveniently written

$$V - \langle V \rangle = \frac{1}{2} \sum_l \lambda_{\text{TA}} \psi_{\text{TA}}^2(l),$$

where λ_{TA} is the disorder parameter which can be calculated for the TA vibrations.

$$\lambda_{\text{TA}} = \left(1 + \frac{l_1}{l_2} \right)^{-2} \left[2(A+B)\Delta_1 - 8B_2 \left(\frac{l_1}{l_2} \right) \right]$$

$$\approx 1 \times 10^3 \text{ sec}^{-2},$$

with

$$\frac{\bar{l}_1}{\bar{l}_2} = \frac{4B}{m_{zn}} \frac{1}{(\omega_{\text{TA}}^2 - 4A/m_{zn})}.$$

The calculated localized frequency $(\omega_{\text{TA}}^2 + \lambda_{\text{TA}})^{1/2} = 80 \text{ cm}^{-1}$ is in good agreement with the experimental value $\text{TA}_X(\text{ZnS}) = 83 \text{ cm}^{-1}$.

This interpretation which has been proposed to explain the behavior of the acoustical branches can

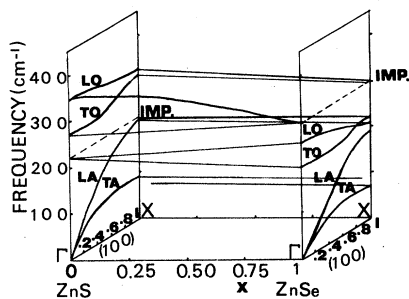


FIG. 5. Frequency dependence of the ZCP and ZEP in the direction $\langle 100 \rangle$ as a function of the concentration x ; IMP are the impurity-localized and gap modes of S in ZnSe and Se in ZnS, respectively.

be extended to the optical branches and explains why no cross-coupling between optical ZEP has been observed. The second part of our discussion will be devoted to a phenomenological discussion of the ZEP behavior in mixed $\text{ZnS}_{1-x}\text{Se}_x$.

In a zinc-blende crystal $AB_{1-x}C_x$ where $m_B < m_A < m_C$, the LO and LA ZEP in the directions of alternating planes are respectively generated by displacements of either the A or B atoms in the crystal AB, and by the A or C atom displacements in the crystal AC. The atom A generates the LA zone-edge mode of the crystal AB and the zone-edge LO mode of the crystal AC. We should then expect the LA phonon of AB to become the LO phonon of AC with increasing C concentration.

The vibrations of the light (S) and heavy (Se) foreign impurity atoms in AC (ZnSe) and AB (ZnS) crystals, respectively, give rise to a local and a gap nonpropagating mode. They will be the frequencies toward which will merge all the optical branches from all the points, and from all the di-

rections of the BZ when the content of B or C decreases. This behavior can be generalized to all mixed crystals where localized and gap modes appear.

In Fig. 5 the result of our discussion is shown in the direction $\langle 100 \rangle$. The dispersion curves of pure ZnS and ZnSe are taken from Refs. 11 and 12. The optical branches merge into the impurity mode with decreasing S(Se) concentration, the LA (ZnS) branch transforms itself into a LO (ZnSe); the TA branches of both constituents remain almost nonmodified as the concentration changes. The ZnS and ZnSe ZEP are seen together with the disorder-induced phonon density of states which is essentially composed of the ZnS TA peak.

CONCLUSIONS

Using ir and RS techniques, it has been possible to study the ZEP behavior of mixed $\text{ZnS}_{1-x}\text{Se}_x$ as a function of x . The behavior of the acoustical branches has been explained by the existence of a localized mode which is added to the virtual-lattice-acoustical branch.

In a zinc-blende-structure $AB_{1-x}C_x$ mixed crystal when $m_B < m_A < m_C$, the LA branch of the AB crystal becomes the LO branch of the AC one; the other optical phonons should tend towards the localized or the gap mode when the impurity concentration is reduced.

ACKNOWLEDGMENT

It is a pleasure to thank Professor O. Brafman and Doctor Z. Vardeny for many helpful discussions and suggestions.

¹R. J. Elliott, J. A. Krumhansl, and P. L. Leath, *Rev. Mod. Phys.* **46**, 465 (1974).

²C. H. Perry, I. R. Jahn, V. Wagner, W. Bauhofer, L. Genzel, and J. B. Sololoff, in *Proceedings of the International Conference on Lattice Dynamics, Paris, 1977*, edited by M. Balkanski (Flammarion, Paris, 1978), p. 419.

³R. Beserman, M. Zigone, W. Drexel, and C. Marti, *Solid State Commun.* **18**, 419 (1976).

⁴R. Beserman, *Solid State Commun.* **23**, 323 (1977); R. Beserman and D. Schmeltzer, *ibid.* **24**, 793 (1977).

⁵B. Ulrici and E. Jahne, *Phys. Status Solidi B* **86**, 517 (1978).

⁶T. Deutch, in *Proceedings of the International Conference on the Physics of Semiconductors, Exeter, 1962*, edited by A. C. Stickland (The Institute of Physics and the Physical Society, London, 1962), p. 50.

⁷R. Marshall and S. S. Mitra, *Phys. Rev.* **134**, A1019

(1964).

⁸S. S. Mitra, *Phys. Rev.* **132**, 986 (1963).

⁹W. G. Nielsen, *Phys. Rev.* **182**, 838 (1969).

¹⁰J. C. Irwin and J. Lacombe, *Can. J. Phys.* **50**, 2596 (1972).

¹¹N. Vagelatos, D. Wehe, and J. S. King, *J. Chem. Phys.* **60**, 3613 (1974).

¹²B. Hennion, F. Moussa, G. Pepy, and K. Kunc, *Phys. Lett.* **36A**, 376 (1971).

¹³O. Brafman, I. F. Chang, G. Lengyel, S. S. Mitra, and E. Carnall, Jr., *Phys. Rev. Lett.* **19**, 1120 (1967).

¹⁴L. Genzel and W. Bauhofer, *Z. Phys.* **B25**, 13 (1976).

¹⁵J. L. Birman, *Phys. Rev.* **131**, 1499 (1963).

¹⁶J. L. Birman, in *Encyclopedia of Physics*, edited by S. Flügge (Springer, New York, 1974), Vol. XXV/2b, Appendix D.

¹⁷K. Kunc, Ph.D. thesis, Paris, 1973 (unpublished); *Ann. Phys. (France)* **8**, 319 (1973/74).

¹⁸M. Balkanski, C. Hirlimann, and J. F. Morhange, in *Proceedings of the International Conference on Lattice Dynamics, Paris, 1977*, edited by M. Balkanski (Flammarion, Paris, 1977), p. 174.

¹⁹O. Brafman and S. S. Mitra, in *Proceedings of the International Conference on Light Scattering in Solids, Paris, 1971*, edited by M. Balkanski (Flammarion, Paris, 1971), p. 284.

²⁰J. Ruvalds and A. Zawadowski, in *Proceedings of the Second International Conference on Light Scattering in Solids, Paris, 1971*, edited by M. Balkanski (Flammarion, Paris, 1971), p. 29.

²¹Z. Vardeny and O. Brafman, *Phys. Rev. B* 12, 3290 (1979).

²²D. Schmeltzer and R. Beserman (unpublished).